Results from a TPC Prototype with MWPC Endcap for the Linear Collider Tracker (DraftNo.27/7Feb2009)

K. Ackermann [c], S. Arai [i], D.C. Arogancia [f], A.M. Bacala [f], M. Ball [a], T. Behnke [a], V. Eckardt [c], K. Fujii [ℓ], N. Ghodbane [a], H.C. Gooc Jr. [f], T. Kijima [i], M. Hamann [a], M. Habu [i], R.-D. Heuer [b] K. Ikematsu [a], A. Kaukher [d], H. Kuroiwa [ℓ], M.E. Janssen [a], Y. Kato [g], M. Kobayashi [ℓ], T. Kuhl [a], T. Lux [b], T. Matsuda [ℓ], A. Miyazaki [i], K. Nakamura [i], O. Nitoh [i], R.L. Reserva [f], N. Sakamoto [h] T. Sanuki [j], R. Settles [c], A. Sugiyama [h], T. Takahashi [e], T. Watanabe [k], P. Wienemann [a], R. Wurth [a], M. Yamaguchi [h], A. Yamaguchi [m], T. Yamamura [j], H. Yamaoka [ℓ]

[a] *DESY Hamburg, D-22607 Hamburg, Germany*
[b] *Universität Hamburg, D-22761 Hamburg, Germany*
[c] *Max-Planck-Institut für Physik, D-80805 Munich, Germany*
[d] *Universität Rostock, D-18051 Rostock, Germany*
[e] *Hiroshima University, Higashi-Hiroshima, Hiroshima 739-8526, Japan*
[f] *Mindanao State University, Iligan City 9200, Philippines*
[g] *Kinki University, Higashi-Osaka, Osaka 577-8502, Japan*
[h] *Saga University, Honjo, Saga 840-8502, Japan*
[i] *Tokyo University of Agriculture and Technology, Koganei, Tokyo 184-8588, Japan*
[j] *University of Tokyo, ICEPP, Tokyo 113-0033, Japan*
[k] *Kogakuin University, Hachiohji, Tokyo 192-0015, Japan*
[ℓ] *KEK, IPNS, Tsukuba, Ibaraki 305-0801, Japan*
[m] *University of Tsukuba, Tsukuba, Ibaraki 305-8577, Japan*

Abstract

A Time Projection Chamber is being investigated as central tracker for a detector at the International Linear Collider. To provide a comparison and explore the potential improvements using Micro-Pattern Gas Detectors compared with Multi-Wire Proportional Chambers used up to now in TPCs, a small prototype chamber capable of being equipped with different gas-amplification techniques was built at MPI-Munich and exposed to cosmics in the 5 T magnet at DESY and subsequently to a testbeam in a 1 T magnet at KEK. The chamber was operated with four different endplate technologies during four beam periods in 2004–2005. This paper reports on results from the first tests using MWPC gas-amplification.

Key words:
International Linear Collider (ILC), Time Projection Chamber (TPC), Multiwire Proportional Chamber (MWPC), Micropattern Gas Detector (MPGD)

PACS: 29.40.Cs, 29.40.Gx

1. Introduction

A detector at the International Linear Collider [1] will have a high-precision tracking system inside a calorimeter system, and both systems will have very high granularity. These will be contained in the detector solenoid which will produce the high magnetic field ($\sim$ 4T) needed to reduce backgrounds at the vertex and to enable very good momentum resolution.

There are two important aspects for tracking at the ILC. The first is, as required by precision-physics measurements at the linear collider, that the detector must determine the momentum of charged tracks an order of magnitude more precisely than in previous experiments. The second aspect is that the detector must be optimized for the reconstruction of multi-jet final states. The jet-energy resolution using the particle-flow technique [2] is best when the reconstruction of individual particles in jets is as complete as possible, which means that efficiency in finding the charged tracks should be as high as possible.

A Time Projection Chamber (TPC) is a candidate for the central tracker because of its very good performance in past collider experiments[3]. In order to obtain the order-of-magnitude improvement in momentum resolution and the highest possible track-recognition efficiency, the LCTPC groups [4] are pursuing R&D to find the best state-of-the-art technology for the TPC.

2. The present series of R&D tests

TPCs have employed Multi-Wire-Proprotional-Chamber (MWPC) gas-amplification in previous large collider detectors. The thrust of the R&D program [4][5] is to develop a TPC based on Micro-Pattern Gas Detectors (MPGDs) which promise to have better point and two-track resolution than wire chambers and to be more robust in high backgrounds. In the present series of experiments, several techniques were compared, gas amplification using MWPC, Micromegas (Micro-mesh gaseous structure)[6] and GEM (Gas Electron Multiplier)[7], and the resistive-anode technique[8].

To research the performance of these technologies, a small prototype chamber was built at MPI-Munich, initially with an MWPC endplate, tested using cosmics at DESY in a 5 T magnet and subsequently exposed in four test-beam runs at KEK using MWPC, GEM, Micromegas and resistive-anode endplates in a 1 T magnet. The chamber will be called MP-TPC, for MultiPrototype-TPC, in the related publications. The runs were performed in the following order: MWPC (January-June 2004), GEM (April 2005), Micromegas (June 2005) and MPGD with resistive anode (October 2005).

The Micromegas results have been published [9], and the other papers are in preparation. Preliminary results have been shown at various workshops (see for example [10]).

The present paper describes the MWPC results. The following paper in this journal presents[11] the GEM results. The MWPC option has been kept as backup solution, since it is a well proven technique, until the MPGD options are more thoroughly understood. However, a new aspect that had to be measured for a TPC with MWPC endplate is how it behaves in a high magnetic field. This property will become evident in this paper which is organized as follows.

The prototype with MWPC and the tests are described in the Sec. 3, the analyses in Sec. 4, results are presented in Sec. 5 and conclusions are drawn in Sec. 6.

3. The MP-TPC chamber

The chamber with MWPC endplate used January-June 2004 is shown in Fig. 1. It has a sensitive length of 257 mm and sensitive diameter of 152 mm. Its outer diameter of 270 mm was designed to fit into the superconducting 5 T magnet at DESY.

The MWPC endcap had significantly reduced pad size, wires-to-pads and wire-to-wire spacing to improve the achievable point and two-track resolutions. The gas amplification occurred at the plane of anode sense wires with 20 μm diameter and spaced with 2 mm pitch. The sense-wire plane

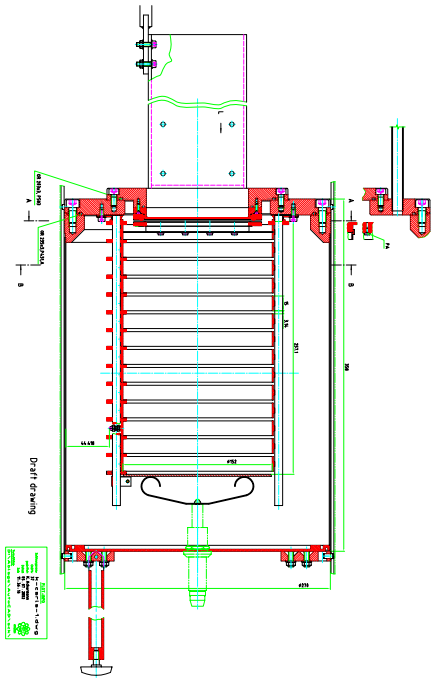

Fig. 1. The MP-TPC prototype with MWPC used for these studies. The cathode is at the bottom and the MWPC anode wires at the top. The 13 fieldcage potential rings which define the drift volume form the ladder-like pattern in the drawing. The fieldcage defines the TPC sensitive volume, and the whole structure is embedded in a cylindrical gas container dimensioned to fit in the 5 T magnet at DESY seen in Fig. 2 (upper).

was placed 1 mm above the pad plane (2 mm–4 mm in previous TPCs). The pads with 2.3 mm×6.3 mm pitch covered the 10 cm×10 cm pad plane.

3.1. *The DAQ system*

The pads were read out with modules based on electronics developed for the TPC of the ALEPH experiment at LEP [12][13]. The pad signals were digitized by an eight-bit FADC running at a clock frequency of 12.5 MHz The electronics available for these tests was able read out up to 384 pad channels. More details of the DAQ system are given in [9].

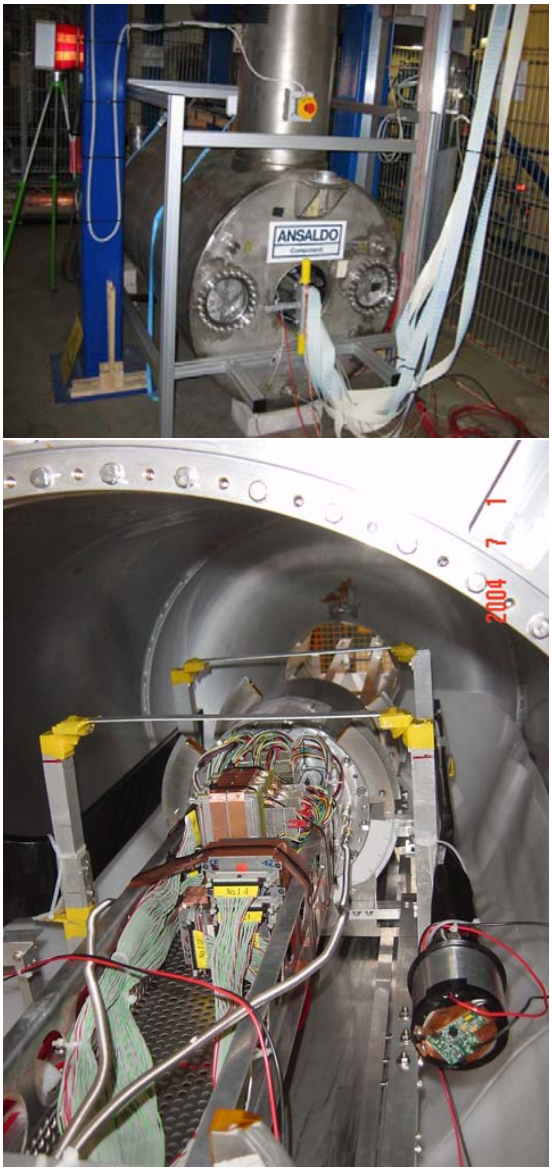

Fig. 2. Upper: The MP-TPC inside the 5 T solenoid at DESY. Lower: The chamber inside the 1 T PCMAG at KEK.

3.2. *The tests with cosmics at DESY and beam at KEK*

The chamber with MWPC and readout electronics were initially commissioned at MPI-Munich and DESY and then installed in the 5 T solenoid as shown in the upper photograph of Fig. 2.This

magnet has a bore diameter of 27 cm and length of 1 m and was equipped with a cosmic-ray trigger. Cosmic data was taken for B-fields between 0 T and 5 T.

After the cosmic runs at DESY, the chamber was transported to KEK where it was installed in the 1 T magnet, seen in the lower photograph of Fig. 2, which was situated in the $\pi 2$ beam line at the KEK 12-GeV PS. The 1 T Persistent Current solenoidal Magnet (PCMAG) [14] has a bore diameter of 85 cm, length of 1.3 m and very thin coil windings with 20 % X_0 thickness.

For the tests with MWPC, a total of $\sim 2 \times 10^5$ cosmic triggers at DESY were registered for B=0 T, 1 T and 4 T, and $\sim 0.5 \times 10^5$ triggers under many different conditions were taken at KEK during the beam runs with B=0 T and 1 T.

3.3. *The $\pi 2$ beamline*

The $\pi 2$ beam provided a secondary beam of electrons, pions and protons with momenta up to 4 GeV/c derived from the PS beam incident on a Be target. The beam spill had a flat top of 1.5 s and a repetition rate of 0.25 Hz.

The beam elements are shown in Fig. 3. Four

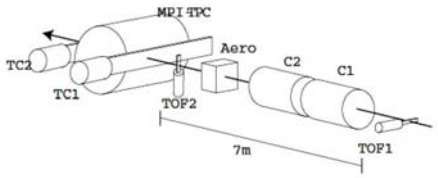

Fig. 3. pi2 beam set up

scintillation counters were used with 4-fold coincidence to trigger the data acquisition. The first two (not shown in the figure) were placed just downstream of the beam slit which controlled the intensity while the second two were located just upstream and downstream of the MP-TPC inside of PCMAG. These counters had an overlap region of $30 \times 10\,\mathrm{cm}^2$ to match the drift region of the chamber. Further details are covered in [9].

In addition, for the MWPC running there were two time-of-flight counters and one aerogel counter (n = 1.03) which allowed the particle identifcation of pions and protons at trigger level. These were employed for the dE/dx measurements described below. There were also two gas-Cherenkov counters for identification of electrons, which, however, were not included in the present analysis.

4. Resolution studies

The diffusion constant C_D is important for the single-point and two-track resolutions and was measured using the behaviour of signal-charge spread as a function of drift distance z. In the simplest model, the r.m.s. of the charge spread (also called "Pad Response") is parametrized by

$$\sigma^2_{PR}(z) = \sigma^2_{PR}(0) + C^2_D \times z, \qquad (1)$$

and the point resolution by

$$\sigma^2_x(z) = \sigma^2_0 + C^2_D/N_{eff} \times z. \qquad (2)$$

The width $\sigma_{PR}(0)$ of the MWPC signal induced on the pads at $z = 0$ is related to geometrical properties at the wire-chamber cell: wire pitch, pad–wire distance and pad size.

The point resolution σ_0 is related to signal-to-noise: electronics and signal-charge spread at $z = 0$. The quantity N_{eff} is the effective number of electrons contributing to the resolution as determined by primary ionization statistics, gain fluctuations and the electronics performance [9][15]. These quantities are also affected by the crossing-angles of the projected track relative to the pads and, in the case of MWPC, relative to the wires.

The charge width was drived from a Gaussian fit to the distribution of charge around the center-of-gravity of a hit. The point resolution was calculated using the Double-Fit program [16] in which standard deviations of hits for a pad row are calculated twice with respect to track-fits ("Double-Fit"), first with and second without the given pad row. The correct point resolution is the geometric mean of the standard deviations of hits with respect to the two fits [17].

Equations 1 and 2 represent the ideal situation and give reasonable agreement with the mea-

surements for a TPC with MPGD gas amplification [9][15]. In the MWPC case, however, $E \times B$ effects are not taken into account completely in these equations, as will be decsiribed next in Sec. ??.

5. Results

The gas used was the so-called TDR gas[2], Ar-CH_4-CO_2 (93:5:2)%. The chamber was operated at atmospheric pressure; the pressure and the ambient temperature were continuously monitored. The drift velocity was measured to be $4.52 \pm 0.04\,\mathrm{cm}/\mu\mathrm{s}$ at the drift field of $220\,\mathrm{V/cm}$ during the beam runs.

5.1. *Charge spread and point resolution*

The cosmic data at B = 0 T, 1 T and 4 T will be compared with 4 GeV/c π^- beam data at 0 T and 1 T magnetic fields. After the data was corrected for dead channels and edge effects, the tracking efficiency was essentially 100%.

Angle cuts of (polar, azimuthal)=($\pm 30^o$, $\pm 3^o$) were applied to the cosmic data to obtain a sample with track directions for comparison with the beam data at (polar, azimuthal)=(0^o, 0^o). The final samples selected for the diffusion and point-resolution comparisons contained about 2×10^4 tracks in the cosmic data and 10^4 tracks in the beam data.

The two plots of Fig. 4 compare the charge width σ^2_{PR} versus z for the DESY cosmic data and the KEK beam data. Figure 5 shows the point resolution σ_x versus z for the two data sets. The fits to the data in Figs. 4 and 5 yeild the parameters in Table 1.

Runs	B(T)	No.tracks	C_D	$\sigma_{PR}(0)$	$\frac{C_D}{\sqrt{N_{eff}}}$	σ_0
Cosmics	0	5986	491±2	1120±6	126± 4	181±19
Cosmics	1	4578	226±2	1240±4	54± 3	206±11
Cosmics	4	9246	112±3	1390±4	0±21	312± 4
Beam	0	5063	466±1	1340±3	117± 3	179±12
Beam	1	5221	212±1	1290±1	48± 2	182± 7

Table 1
Parameters fit to the data. The units are $\mu\mathrm{m}/\sqrt{\mathrm{cm}}$ for C_D and μm for $\sigma_{PR}(0)$ and σ_0.

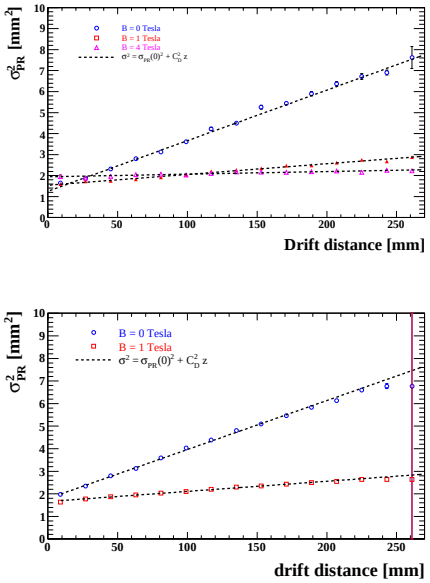

Fig. 4. Diffusion results for DESY cosmics (upper) and KEK beam (lower).

The z resolution was also determined for all data sets, and was consistent with $\sim$0.4–0.5 mm in all cases; an example shown in Fig. 6.

In general the results in Table 1 from the DESY and KEK runs agree to better than $\sim$10%, which is quite reasonable given the very different data-taking environments. The final results will therefore be given by the weighted average of the two runs. Systematic errors equal to one-half the difference between the DESY and KEK periods are assigned to the B=0 T and 1 T averages. Estimated this way, the systematics dominate the statistical errors by about an order of magnitude in almost all cases. Therefore the statistical errors in Table 1 in general significantly underestimate the total error. The total error is therefore taken to be the quadratic sum of statistical and systematic errors.

For the 4 T data, there is no possibility to compare between the two periods to estimate the systematic effects which are dominant as just explained. Since these effects must be included, the average of systmatic errors estimated at 0 T and 1 T are applied to the 4 T data, i.e., $\sigma_{sys-4\mathrm{T}} = \langle \frac{\sigma_{sys}}{\sigma_{stat}} \rangle_{0\mathrm{T},1\mathrm{T}} \times \sigma_{stat-4\mathrm{T}}$, the average being calculated separately for each column 3 to 6 in Table 1.

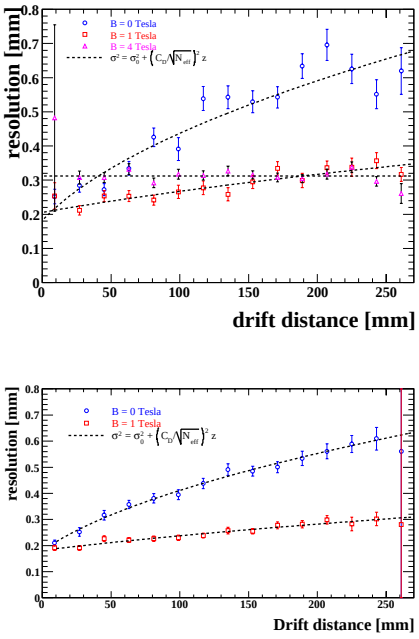

Fig. 5. Point-resolution results for DESY cosmics (upper) and KEK beam (lower).

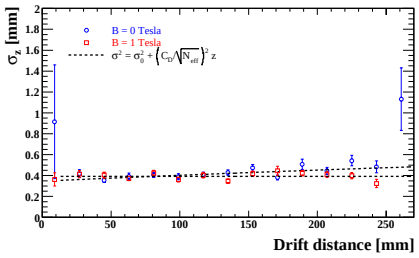

Fig. 6. z resolution for beam data taken at KEK at 1 T.

The resulting averages and total errors are shown in Table 2.

B(T)	C_D	$\sigma_{PR}(0)$	$\frac{C_D}{\sqrt{N_{eff}}}$	σ_0
0	471±12	1296±110	120± 5	180±10
1	215± 7	1287± 25	50± 3	189±13
4	112±33	1390±133	0±44	312± 6

Table 2
Averaged results. The units are $\mu\mathrm{m}/\sqrt{\mathrm{cm}}$ for C_D and μm for $\sigma_{PR}(0)$ and σ_0.

In the case of Fig. 4, the measured C_D values predicted by Magboltz [22] agree with the measured values in Table 2 at 0 T and 1 T, namely 440 and 200 $\mu\mathrm{m}/\sqrt{\mathrm{cm}}$ respectively.

The prediction for B = 4 T, where Magboltz expects 60 $\mu\mathrm{m}/\sqrt{\mathrm{cm}}$, is lower than the measurement by about 1.5 standard deviations of total error, but it is too small by many standard deviations of statistical error. This fact was perplexing at first since the Magboltz value seems to be correct [23][24]. Thus initially a search was performed throughout the data/analysis chain to see if a bias in the measurement could explain the difference. No such bias could be identified, and finally the difference is attributed here to systematic effects as given in Table 2.

The slopes in Fig. 5 correspond to N_{eff} values in Eq. 2 of 15.4±1.5 for B = 0 T. and 18.5±2.5 for B = 1 T. At 4 T, a value for N_{eff} cannot be given obviously, and this result will be discussed next.

At 4 T one might expect $\frac{C_D}{\sqrt{N_{eff}}}$, in a simple model where N_{eff} is the same at 1 T and 4 T, to be about one quarter of that at 1 T, i.e. around $12\,\mu\mathrm{m}/\sqrt{\mathrm{cm}}$. This expectation is consistent with the measurement at 4 T since it is well within the error. The flatness of the curve at 4 T in Fig. 5 was somewhat of a mystery, and a toy Monte Carlo was used to help understand it. The study showed that the $E \times B$ influence at large B decreases as a function of increasing drift distance z because the diffusion becomes dominant. The combination of the two effects combine to produce a nearly flat behaviour as seen in Fig. 5.

5.2. *Angle effect*

To measure the angular dependence, the MP-TPC was rotated by angles ϕ with respect to the beam direction of $\phi \approx \pm 10^0$ and $\pm 20^0$ and exposed for roughly 10^3 triggers to the π beam at 4 GeV/c. The results [18] for $\sigma_{PR}(0)$ are shown in Fig. 7. The shape of this curve is a measure of the pad-angle effect and is proportional to $\frac{h \cdot \tan\varphi}{\sqrt{12 \cdot N_{eff}}}$, where h is the pad height.

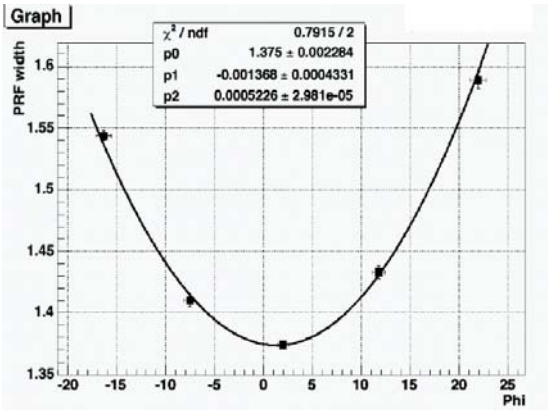

Fig. 7. Angle dependence of the pad response.

5.3. *dE/dx studies*

The trigger elements are described in Sec. 3.2. The proton and π^- at 1, 2 and 4 GeV/c were used for the dE/dx results [19][20]. Figure 8 shows dE/dx results, and Fig. 9 the measured $\beta\gamma$ dependence of dE/dx.

The dE/dx accuracy was measured to be between 22% and 27% for the MP-TPC. When extrapolated to the size of the LCTPC, these correspond to an accuracy of 3.6% to 4.2%. Thus an important TPC by-product for the linear collider physics analyses, the dE/dx performance for particle identification, has been verified at these testbeam runs.

6. Conclusions

The MWPC point resolution is unfavorably affected by E×B effects for large magnetic field, as clearly seen in Fig. 5. With MWPC the point error measured at 4 T is about a factor three larger than the goal for the LCTPC [4], so that the previously successful MWPC technology in past experiments is no longer considered to be the best option for the TPC at the linear collider.

The following paper in this issue of NIM[11] describes the very positive results at the KEK testbeam using a GEM[7] endcap on the MP-TPC prototype.

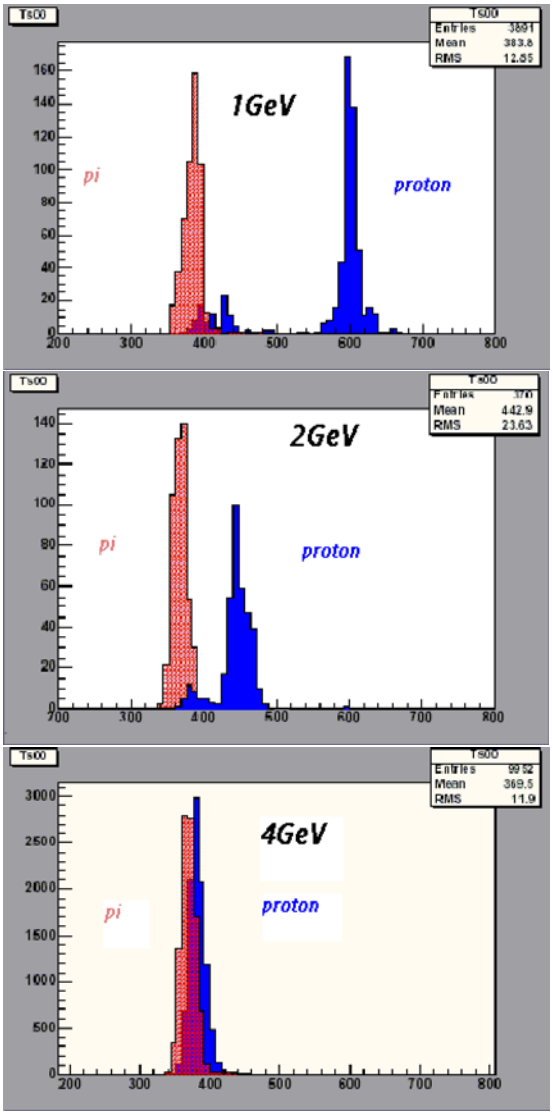

Fig. 8. Measured dE/dX-distributions.

References

[1] The GDE (Global Design Effort) submitted the initial design for the complete ILC machine in 2007. This "Reference Design Report" is available at http://www.linearcollider.org/rdr.

[2] TESLA Technical Design Report, DESY 2001-011, ECFA 2001-209, March 2001.

[3] M.T. Ronan, *Time-projection chambers*, p.264 of the PDG Particle Physics Booklet July 2004. For a thorough overview of TPC applications, see

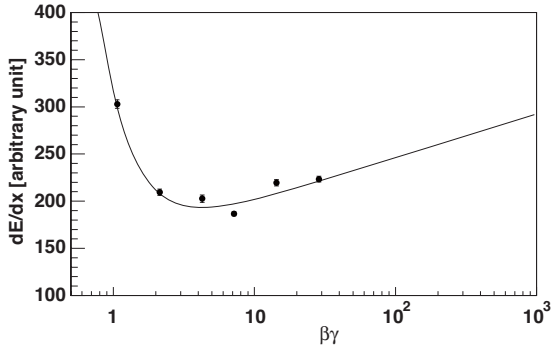

Fig. 9. $\beta\gamma$ dependence

http://instrumentationcolloquium.lbl.gov /Time_Projection_Chamber_R&D.pdf.

[4] The TPC status report to the Tracking Review by the WWS R&D Panel at the ACFA LC workshop in Beijing, February 2007, included a complete overview of the groups, of design issues for the LCTPC and of the R&D work to address the issues. It is published as LC Note LC-DET-2007-005 at http://flcweb01.desy.de/lcnotes.

[5] Proposal PRC R&D-01/03, DESY Physics Review Committee October 2001, published as LC Note LC-DET-2002-008 at http://flcweb01.desy.de/lcnotes. See http://www.desy.de/f/prc/ for the October 2001, May 2003, November 2005, May 2006 and April 2008 R&D status reports.

[6] Y. Giomataris et al., *Micromegas: A High Granularity Position Sensitive Gaseous Detector for High Particle Flux Environments*, Nucl. Instr. and Meth. A376(1996)29.

[7] F. Sauli, *GEM: A New Concept for Electron Amplification in Gas Detectors*, Nucl. Instr. and Meth. A386(1997)531.

[8] M. Dixit et al., Nucl. Instr. and Meth. A518(2004)721. See also www.physics.carleton.ca/research/ilc/tpc.html.

[9] D. C. Arogancia et al., *Study in a beam test of the resolution of a Micromegas TPC with standard readout pads*, http://arxiv.org/pdf/0705.2210, submitted to Nucl. Instr. and Meth. (2007).

[10] M. Kobayashi et al., Nucl. Instr. and Meth. A581(2007)265 and references therein.

[11] K. Ackermann et al., Nucl. Instr. and Meth. A???(200?)???, *Results from a TPC Prototype with GEM Encap for the Linear Collider Tracker*, following paper in this issue of Nucl. Instr. and Meth.

[12] M. Ball, N. Ghodbane, M. Janssen and P. Wienemann, *A DAQ System for Linear Collider TPC Prototypes based on the ALEPH TPC Electronics*, LC-DET-2004-013 at http://flcweb01.desy.de/lcnotes.

[13] C. Bowdry, ed., The Aleph Handbook (1995), ISBN 92-9083-072-7, publ. by CERN 1995.

[14] Y. Ajima et al., *A superconducting solenoidal spectrometer for a ballon-borne experiment*, Nucl. Instr. and Meth. A443(2000)71.

[15] M. Kobayashi, *An estimation of the effective number of electrons contributing to the coordinate measurement of a TPC*, Nucl. Instr. and Meth. A562(2006)136.

[16] M.E. Jannsen, *Auflösungsstudien an einer Zeit-Projektions-Kammer (TPC) mit GEM-Gasverstärkungssystem*, Diplomarbeit U.Dortmund, DESY-THESIS-2004-049, September 2004.

[17] This application of the geometric-mean for this measurement has been used for several years; a recent proof is given in the appendix of Ref. [9].

[18] K. Nakamura, thesis, Tokyo University of Agriculture and Technology.

[19] S. Arai, *Measurement of energy loss by charged particles with a Time Projection Chamber*, Diploma thesis 2005, Tokyo U. of Argiculture and Technology, Japan.

[20] R.L. Reserva, presented at the LCWS2005, Stanford University.

[21] S.R. Amendolia et al., *The spatial resolution of the ALEPH TPC*, Nucl. Instr. and Meth. A283(1989)573-577.

[22] S.F. Biagi, Nucl. Instr. and Meth. A283(1989)716.

[23] J. Kaminski et al., *Developent and studies of a time projection chamber with GEMs*, Nucl. Instr. and Meth. A535(2004)201-205.

[24] D. Karlen et al., *TPC performance in magnetics fields with GEM and pad readout*, Nucl. Instr. and Meth. A555(2005)80-92.